Polypropylene–Bamboo/Glass Fiber Hybrid Composites: Fabrication and Analysis of Mechanical, Morphological, Thermal, and Dynamic Mechanical Behavior

SUSHANTA K. SAMAL, SMITA MOHANTY
AND SANJAY K. NAYAK*

Laboratory for Advanced Research in Polymeric Materials (LARPM)
Central Institute of Plastics Engineering and Technology
Bhubaneswar 751 024, India

ABSTRACT: Hybrid composites of polypropylene reinforced with bamboo and glass fibers (BGRP) were fabricated using an intermeshing counter rotating twin screw extruder followed by injection molding. Maleic anhydride grafted polypropylene (MAPP) has been used as a coupling agent to improve the interfacial interaction between the fibers and matrix. The mechanical properties of the hybrid composites were studied from tensile, flexural, and impact tests. Mechanical tests indicated an increase in tensile, flexural, and impact strength of the BGRP hybrid composites at a bamboo:glass fiber ratio of 15:15 ratio in the presence of 2 wt% of MAPP. Nearly, 69, 86, and 83% increase in tensile flexural and impact strength respectively has been observed as compared with virgin PP. The fiber matrix interfacial morphology of the tensile fractured specimens was studied using scanning electron microscopy (SEM) which showed less fiber pullout and comparatively less gaps between the fiber and the base matrix in the case of MAPP treated hybrid composites. The crystallization, melting behavior and thermal stability of the hybrid composites were investigated employing differential scanning electron microscopy (DSC) and thermogravimetric analysis (TGA). Thermogravimetric analysis (TGA) showed an increase in thermal stability of the matrix polymer with incorporation of bamboo and glass fibers, confirming the effect of hybridization and efficient fiber matrix interfacial adhesion. The dynamic mechanical analysis (DMA) showed an increase in storage modulus (E') indicating higher stiffness in case of hybrid composites as compared with untreated composites and virgin matrix. The tan δ spectra presented a strong influence of fiber content and coupling agent on the α and γ relaxation process of PP.

KEY WORDS: PP, hybrid composite, MAPP, SEM, TGA, DMA.

INTRODUCTION

SHORT NATURAL FIBERS such as sisal, jute, banana, coir, pineapple leaf fiber (PALF) reinforced thermoplastic composites [1–8] are increasingly gaining attention for

*Author to whom correspondence should be addressed. E-mail: drsknayak@gmail.com
Figures 6–9 appear in color online: http://jrp.sagepub.com

0731-6844/09/22 2729–19 $10.00/0 DOI: 10.1177/0731684408093451

their emerging application in the fields of aerospace, automotives, construction, textiles, etc. Low cost, easy availability, low density, light weight, high strength to weight ratio, less wear and tear in processing machineries, and environmental friendly characteristics of the natural fiber reinforced composites have been the primary benefits for their commercial application. Despite the advantages, use of natural fiber reinforced composites has been restricted due to the high moisture absorption tendency, poor wettability, limited thermal stability during processing, and poor adhesion of the natural fibers with the synthetic counterparts. In order to develop composites with better mechanical properties and environmental performance, it is necessary to impart hydrophobicity to the natural fibers. Various fiber surface treatments such as alkali/mercerization [9,10], silane [11,12], combination of alkali and silane [13,14], monomer grafting under UV radiation [15,16], and various other methods such as acetylation, benzyolation, etc. [17,18] have been reported by several authors. Similarly other methods include incorporation of polar maleic anhydride grafted polypropylene (MAPP) which improves the fiber dispersion and fiber/matrix interfacial interaction through hydrogen bonding between hydroxyl groups of natural fibers and carbonyl groups of the maleic anhydride segment of the MAPP [19–25] thereby reducing the rate of moisture absorption and increasing the mechanical strength in the composites [21–25].

Hybridization allows designers to tailor the composite properties according to the desired structure under consideration [26–29]. The impediments in natural fiber reinforced composites can be balanced by combination with glass fiber to produce hybrid composites with desired attributes that include the optimum characteristics of both the combination along with cost:performance ratio. Intermingled or intimately mixed hybrids, wherein the constituent fibers are mixed as randomly as possible so that no concentrations of either type are present in the material, have gained much popularity. Various attempts have already been made using different synthetic fiber reinforced hybrid composites such as carbon/glass [30–34], carbon/Kevlar [35–38], carbon/UHMPE [39–42], aramid/UHMPE [43,44], and UHMPE/glass [45]. Hybridization of natural fiber with stronger and corrosion resistant synthetic fibers like carbon, aramid, glass, etc., can improve the stiffness, strength, as well as moisture resistance of the composites. However, a few literatures are available on natural/synthetic fiber reinforced hybrid composites [28,46–48]. Kalaprasad et al. [49,50] have studied the low density polyethylene (LDPE) based short banana–glass fiber hybrid composite and have observed a considerable enhancement in the mechanical properties of the composites. Yang et al. [51] studied the mechanical and interfacial properties of banana–glass fiber reinforced PVC hybrid composite and have reported a substantial increase in impact strength.

In the present investigation, an attempt has been made to develop hybrid composite in which the percentage of glass and bamboo fiber in the composites have been varied to evaluate the effect of hybridization on the properties of the composites. The enhancement in mechanical properties of PP reinforced with glass as well as a lignocellulosic bamboo fiber has been examined. Storage modulus (E'), loss modulus (E''), and damping characteristics in the bamboo/glass fiber PP hybrid composites has been studied using dynamic mechanical analysis. The thermal stability in the hybrid composites have also been evaluated using DSC/TGA thermograms. The fiber matrix morphology of the interface region has been investigated employing SEM analysis.

EXPERIMENTAL

Materials

Isotactic polypropylene (Grade M110) obtained from M/s Haldia Petrochemicals, Kolkata with a density of 0.9 g/cm^3 and MFI 11 g/10 min (2.16 kg, 230°C) has been used as the base matrix for this study.

Bamboo fiber (4–6 mm length, diameter 85–120 μm, density 0.863 g/cm^3) and glass fiber (6 mm, density 2.56 g/cm^3) were used as reinforcement. Maleic anhydride grafted PP (MAPP), procured from M/s Eastman Chemicals Ltd. Germany, under the trade name Epolene G-3015 having <1 wt% maleic anhydride, with M_w 47,000 and acid number 15 has been used as coupling agent.

The properties of bamboo and glass fiber is enumerated in Table 1.

Composite Preparation

The bamboo fibers scoured in hot detergent solution (2%) at 70°C for 1 h to remove dirt and core material, followed by washing with distilled water, were dried in a vacuum oven at 70°C for 3 h. The dried fibers were cut to desired length of 4–6 mm. Prior to melt blending both bamboo and glass fibers are predried in a vacuum oven at 70°C for 1 h.

Polypropylene was melt blended with short bamboo fibers at different weight percentage (10, 20, 30, and 40%) in an intermeshing counter rotating twin screw extruder (CTW-100, Haake, Germany) having a barrel length of 300 mm and angle of entry of 90°. The process was carried out at a screw speed of 50 rpm and temperature range of 155, 160, and 170°C between the feed zone to die zone. MAPP was used as a coupling agent to modify the interfacial region between the fiber and the matrix, the concentration of which was varied between 1–3 wt%. Similarly, bamboo/glass fiber reinforced hybrid PP composites were fabricated using various weight percent of bamboo:glass fiber ratio (25:5, 20:10, 15:15, 10:20, and 5:25) at optimized processing conditions of 50–60 rpm and temperature of 155–170°C from feed to die zone with and without MAPP. Finally, these extrudates were cooled in water at room temperature, granulated in a pelletizer (Fisons PP 1, Germany) and dried. These dried granules were taken for preparation of rectangular bars and dumbbell shaped specimens as per ASTM-D using a 80T injection molding machine (ESS 330/80HL, Engel, Austria) having clamping force of 800 kN, with a maximum swept volume 254 cm^3 fitted with a dehumidifier (Bry-Air, USA) at temperature range 60–80°C. The specimens were molded at a temperature range of 160–180°C and 1800 bar injection pressure.

Table 1. Properties of bamboo and glass fiber.

Fiber type	Density (g/cm^3)	Diameter (μm)	Tensile strength (MPa)	Young's modulus (MPa)	Failure strain (%)	Moisture absorption (%)
Bamboo	0.863	5–120	520	35,910	3	9
Glass	2.56	–	2400	70,000	–	–

Characterization Techniques

Tensile and flexural tests of virgin PP, untreated and MAPP treated bamboo fiber reinforced PP composites (BFRP), and bamboo–glass fiber reinforced PP hybrid composites (BGRP) specimens, were conducted using a universal testing machine (Lloyds, LR 100K, UK) according to ASTM-D 638 and ASTM-D 790 respectively. The tensile tests were carried out at a cross-head speed of 50 mm/min and gauge length of 50 mm whereas the flexural tests were conducted at a cross-head speed of 1.3 mm/min and span length of 50 mm. Izod impact strength for the specimens having dimensions $63.5 \times 12.7 \times 3$ mm was determined as per ASTM-D 256 with 'V' notch depth of 2.54 mm and notch angle of 45°, using Impactometer 6545 (Ceast, Italy). Five specimens of each composition were tested and the average values have been reported.

For the water absorption test, rectangular specimens with dimensions of 25.4×76.2 mm were cut from the sheets. Three replicate specimens were tested and the results are presented as an average of the three. The samples were dried in an vacuum oven at 50°C for 24 h, cooled in a desiccator and immediately weighed to the nearest 0.001 g. In order to measure the water absorption of the composites, all samples were immersed in water for about 24 h at room temperature as described in ASTM D 570–99 (ASTM 1999) procedure. Excess water on the surface of the samples was removed before weighing. The percentage increase in weight during immersion was calculated to the nearest 0.01% as follows:

$$\text{increase in weight } \% = \frac{\text{wet wt.} - \text{reconditioned wt.}}{\text{reconditioned wt.}} \times 100.$$

Dynamic mechanical properties were assessed using a dynamic mechanical analyzer (model DMA-VA-4000, Germany). A double cantilever clamp was used in a bending mode. The measurements were carried out using the injection molded specimen under nitrogen atmosphere at a scanning rate of 2°C/min from –150 to 150°C with a fixed frequency of 1 Hz and an oscillation amplitude of 0.15 mm.

Differential scanning calorimetry (DSC) experiments were recorded using a Perkin–Elmer Diamond DSC-7 calorimeter at a heating rate of 10°C using approximately 5–10 mg of sample under nitrogen atmosphere. This process consisted of a first heating scan from 40 to 200°C at a heating rate of 10°C, followed by an isothermal step at 200°C for 1 min to eliminate the previous thermal history with a subsequent cooling scan to 40°C at a heating rate of 10°C and final second heating step up to 200°C respectively. Melting temperature (T_m) and enthalpy of fusion (ΔH_f) were measured from DSC heating curve whereas the crystallization temperature (T_c) was taken from the DSC cooling curve. Thermogravimetric analysis (TGA) was carried out employing a Perkin–Elmer Pyris-7. TGA equipment at a heating scan of 10°C from 40 to 500°C under nitrogen atmosphere. The thermal degradation temperature was taken as the minimum of the first derivative of the weight loss with respect to time.

Scanning electron microscope (SEM) observation of the tensile fractured surfaces BFRP composites as well as BGRP hybrid composites with and without MAPP was performed using LEO 1430 VP/LEO model SEM, UK. The fractured surfaces were coated with gold in a BAL-TEC SCD 050 Sputter Coater to avoid electrical charge accumulation.

RESULTS AND DISCUSSION

Mechanical Properties

TENSILE PROPERTIES

Tensile strength and modulus of virgin PP, untreated BFRP composites with bamboo fiber content of 10–40 wt% and MAPP (1, 2, and 3 wt%) treated BFRP composites with 30 wt% of bamboo fiber content are shown in Table 2. It is observed that the tensile strength increases with the increase in bamboo fiber content up to 30 wt% with a subsequent decrease in tensile strength at 40 wt% of fiber loading. However, the tensile modulus increases steadily with the increase in the bamboo fiber content from 10 to 40 wt%. This increase in the tensile strength is attributed to increased wt% of the fiber loading within the matrix leading to an efficient stress transfer from the matrix to the fiber. Tensile strength of BFRP at 30 wt% of fiber loading increases to 21.4% as compared to virgin PP. Deterioration in tensile strength at higher fiber content is a direct consequence of poor fiber/matrix adhesion which leads to micro-crack formation at the interface under loading and non-uniform stress transfer due to the fiber agglomeration in the matrix. Higher wt% of fiber content also leads to an increase in fiber–fiber interaction which results in difficulties in dispersion of the fibers within the polymer matrix. With the incorporation of a compatibilizer (MAPP), a further increase in tensile strength and modulus was observed for all samples compared to the untreated composites at 30 wt% fiber loading. This is primarily due to covalent bonding between the anhydride groups of MAPP and hydroxyl groups of the bamboo fiber along with chain entanglement between MAPP and PP chains that creates a good stress transfer at the interface.

In the case of hybrid composites, the total fiber content was fixed at 30 wt% due to the optimum tensile strength in comparison to other variations. At a total of 30 wt% fiber content, the amount of bamboo fiber was replaced by 5, 10, 15, 20, and 25 wt% of glass

Table 2. Mechanical properties.

Sample type	Bamboo content (%)	Glass content (%)	Tensile strength (MPa)	Tensile modulus (MPa)	Flexural strength (MPa)	Flexural modulus (MPa)	Impact strength (J/m)
PP	0	0	32.03	585.96	35.25	1361.71	32.45
BFRP	10	0	36.32	710.41	37.23	1580.00	41.50
	20	0	38.21	812.57	40.26	1762.35	47.20
	30	0	43.96	1240.20	45.42	1920.75	53.6
	40	0	40.25	1290.82	43.8	1975	48.7
BGRP	25	5	45.47	1311.06	44.21	2100.00	48.00
	20	10	47.22	1380.80	51.51	2275.06	52.16
	15	15	51.00	1426.14	51.20	2300.00	61.50
BFRP+1% MAPP	10	20	48.00	1311.34	48.63	2198.00	59.32
	5	25	39.50	1295	47.31	2019.65	55.00
	30	0	46.65	1425.55	52.30	2096.95	58.26
BFRP + 2% MAPP	0	0	50.18	1685.00	58.00	2271.50	62.25
BFRP + 3% MAPP	30	0	48.50	1550.00	54.26	2085.00	59.50
BGRP + 1% MAPP	15	15	54.50	1491.49	64.5	2662.00	63.50
BGRP + 2% MAPP	5	15	61.40	1685.90	69.3	2910.00	75.90
BGRP + 3% MAPP	15	15	58.25	1520.50	62.60	2745.50	72.00

fiber from BFRP composites. Table 1 shows the variation of their tensile properties of BGRP with and without MAPP. It is observed that the tensile properties of BGRP increases over BFRP, which is mainly due to the replacement of weak and less stiff bamboo fibers with stronger and stiffer glass fibers. The BGRP at 15 wt% each of bamboo and glass fiber loading shows optimum tensile strength as at this composition there is an effective transformation of load from bamboo fiber. At 15 wt% ratio bamboo:glass fibers, the tensile strength of BGRP increased to the tune of 16% in comparison to the pure BFRP at 30 wt% fiber content. Above 15 wt% of glass fiber content, there will be a negative hybrid effect due to the fiber agglomeration. Inclusion of 2 wt% of MAPP to the BGRP hybrid composites prepared at 15:15 wt% of bamboo:glass fibers further enhances the tensile strength and modulus to about 20.4 and 18.21% respectively due the formation of strong covalent linkage between the –OH group of bamboo fiber and SiO group of glass fibers with MAPP thereby resulting in improved interfacial adhesion between the matrix and both types of fibers. However, at higher MAPP concentration of 3 wt%, a marginal decrease in mechanical properties was observed due to the self entanglement of MAPP resulting from the migration of excess MAPP around the fiber surface rather than causing interchain entanglement and contributing to the mechanical continuity of the system.

FLEXURAL PROPERTIES

The variation of flexural strength and modulus of untreated and treated BFRP with different fiber loading is also represented in Table 2. The flexural modulus of BFRP increases linearly with the increase in bamboo fiber content up to a fiber loading of 30 wt%. The flexural strength and modulus of BFRP at 30 wt% bamboo fiber is 22 and 21.6% higher than that of virgin PP matrix. The increased flexural strength of hybrid composites with the glass fiber loading is mainly due to the increased resistance to the shearing of the composites and as a result of the inclusion of rigid glass fiber [50]. However, addition of compatibilizer (1, 2, and 3 wt%), results in an increase in the flexural strength and modulus. BFRP composites prepared at 2 wt% MAPP and 30 wt% of bamboo fiber displays efficient fiber–matrix interfacial adhesion. Variation of flexural properties upon hybridization of glass fiber followed by MAPP treatment is also represented in Table 2. Incorporation of 15 wt% of glass fiber leads to a hybrid effect displaying an increase in flexural strength and modulus to the tune of 12.73 and 19.7%, respectively, as compared to BFRP with 30 wt% of bamboo fiber. The enhancement in the stiffness of the hybrid composites is attributed to similar phenomenon that the modulus of glass fiber is considerably higher than that of bamboo fiber. Further, flexural modulus of hybrid composites increases at 2% of MAPP coupling agent loading, thus continuing the fact that coupling agents are able to synergistically interact with both the fibers and improve the compatibility between them, thereby enhancing the stiffness of the composites and hybrid composites.

IMPACT STRENGTH

The presence of fibers in a composite plays a major role in improving the impact resistance of the matrix. The impact strength of virgin PP and treated and untreated BFRP and BGRP are enumerated in Table 2. A linear increment in the impact strength is observed with addition of bamboo fiber up to 30 wt% due to excellent dispersion of fiber and effective stress transfer between the fiber and the matrix at this composition. At higher fiber loading, fiber to fiber contact increases and breakage of fiber occurs within the composites. This increased fiber to fiber contact reduces the effective stress transfer

between the fiber and matrix, which contributes deterioration in the impact strength at higher fiber loadings. The impact strength at 30 wt% of bamboo fiber loading is 53.6 J/m which increases to 61.50 J/m with the addition of glass fiber to 15 wt%. Nearly 14.74% increase in impact strength was obtained in hybrid composites of bamboo and glass fiber with an equal ratio of 15:15, respectively, due to the synergistic effect of both fibers. Addition of MAPP within BFRP and BGRP, further improves the impact strength due to the flexibility of interface molecular chain resulting in comparatively greater energy absorption.

Water Absorption Behavior

The rate of water absorption depends on the internal material states, nature of fiber constituents, fiber–matrix interface, as well as environmental factors like temperature and applied stress. The effect of fiber and MAPP on percentage of water absorption behavior of BFRP composites and BGRP hybrid composites at 25°C for 24 h was investigated and indicated in Figure 1. The diffusion of water molecules into the matrix can take place by capillary action along the fiber–matrix interface into the bulk resin. Figure 1 clearly indicates maximum percentage of water absorption of BFRP with 30 wt% of bamboo fiber because of high moisture uptake capacity of the bamboo fibers due to the presence of hydrophilic –OH groups in the fibers. Replacement of bamboo fiber with glass fiber decreases the moisture absorption in the hybrid composites due to negligible water absorption capacity of water–impermeable glass fiber as compared to bamboo fiber. Glass fiber acts as a barrier to the bamboo fiber, thus preventing the direct contact between the bamboo fiber and water. However, in case of 2 wt% MAPP treated BFRP (30 wt% of bamboo fiber) and BGRP (15 wt% of bamboo fiber and 15 wt% of glass fiber),

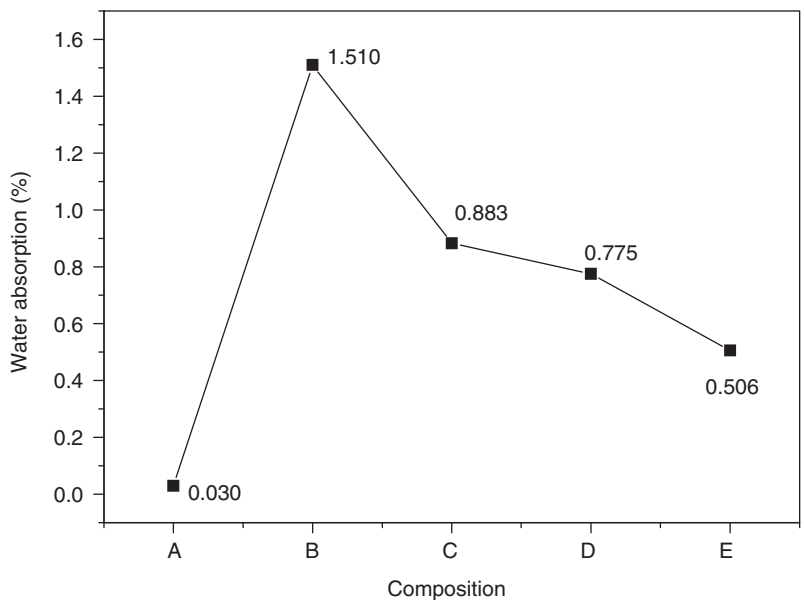

Figure 1. *Water absorption (%) of (a) PP (V), (b) PP + 30%BF, (c) PP + 15%BF + 15%GF, (d) PP + 30%BF + 2%MAPP, (e) PP + 15%BF + 15%GF + 2%MAPP.*

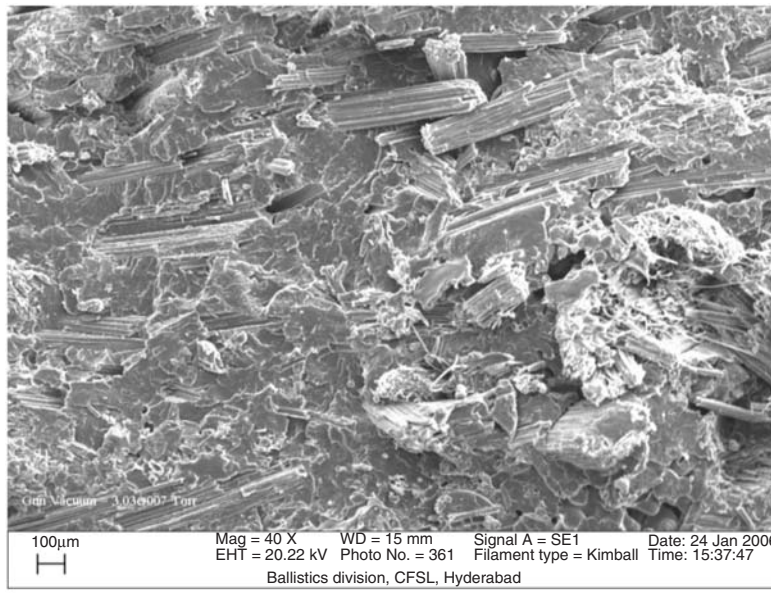

Figure 2. *SEM of PP + 30%BF.*

the water absorption was reduced by 95 and 74.5% as compared to untreated BFRP and BGRP of the same composition, respectively. This can be explained by the improved fiber–matrix interfacial interaction due to the coupling effect of MAPP with –OH groups of bamboo fiber resulting in a less hydrophilic composite. The improved fiber–matrix interfacial bonding also reduces water accumulation in the interfacial voids that prevents water from entering the bamboo fiber.

Morphology

SCANNING ELECTRON MICROSCOPY (SEM)

Fiber–matrix interaction and fracture behavior of treated and untreated BFRP and BGRP can be studied by SEM of the tensile fractured specimen. In the case of BFRP with 30 wt% of bamboo fiber (Figure 2) and BGRP with 15:15 wt% ratio of glass and bamboo fibers (Figure 3), fiber breakage, fiber pull-out, and voids or air entrapments was observed which is a result of poor interfacial bonding between fiber and matrix. The fractured surface of the bamboo/glass-PP hybrid composites showed even more brittle texture with extensive fiber fractures and less fiber pullouts. However, evidence of improved bamboo fiber and PP matrix adhesion can be seen from the MAPP incorporated BFRP (Figure 4) and BGRP (Figure 5) composites in which fiber pull-outs are less extensive. This is mainly because the anhydride group present in MAPP strongly adheres to the –OH on the bamboo fiber surface fiber and the SiO group of the glass fiber. Furthermore, it was also observed that in the case of MAPP treated composites the fibers were pulled out together with the bulk matrix thus confirming efficient interfacial adhesion. The morphological interpretations were in agreement with the mechanical findings which show improved performance characteristics in the MAPP treated BFRP and BGRP composites.

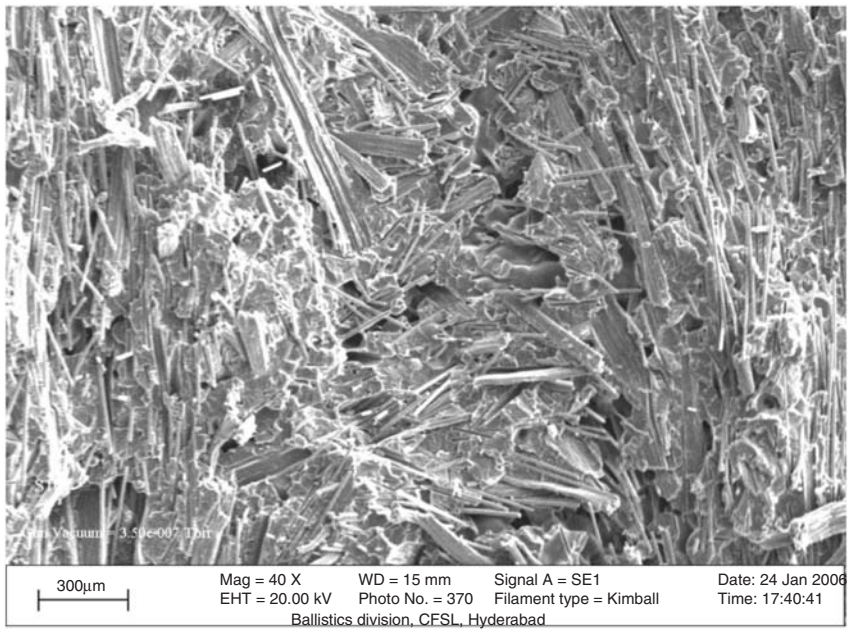

Figure 3. *SEM of PP + 15%BF + 15%GF.*

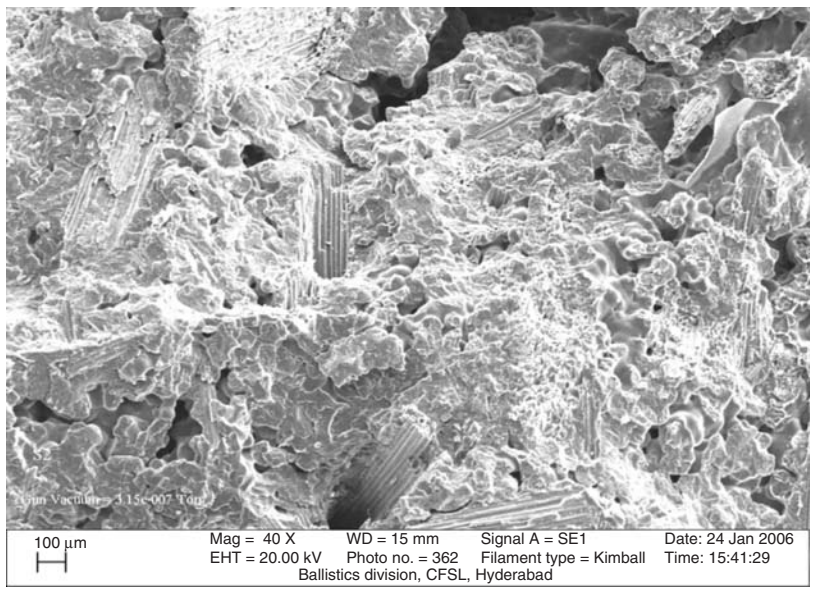

Figure 4. *SEM of PP + 30%BF + 2%MAPP.*

Thermal Properties

DIFFERENTIAL SCANNING CALORIMETRY (DSC)

The melting and crystallization behavior of virgin PP, untreated and 2 wt% MAPP treated BFRP with 30 wt% bamboo fiber and BGRP with 15 wt% of bamboo and glass

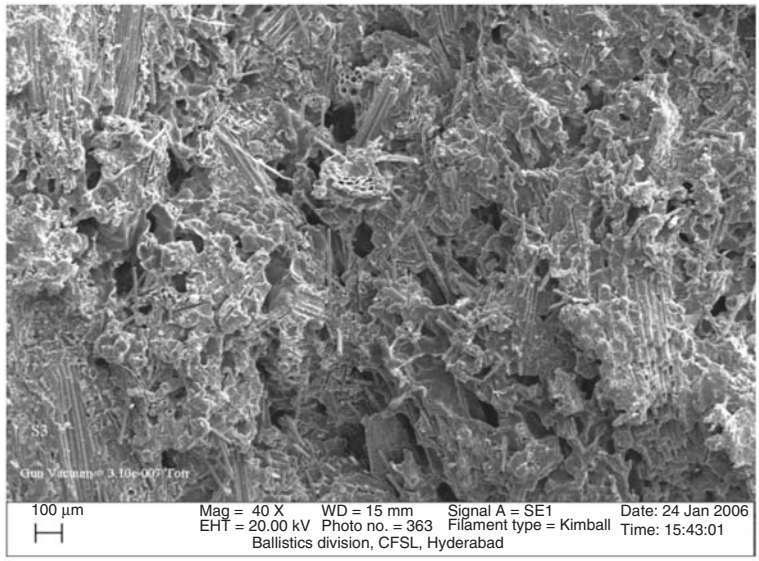

Figure 5. *SEM of PP + 15%BF + 15%GF + 2%MAPP.*

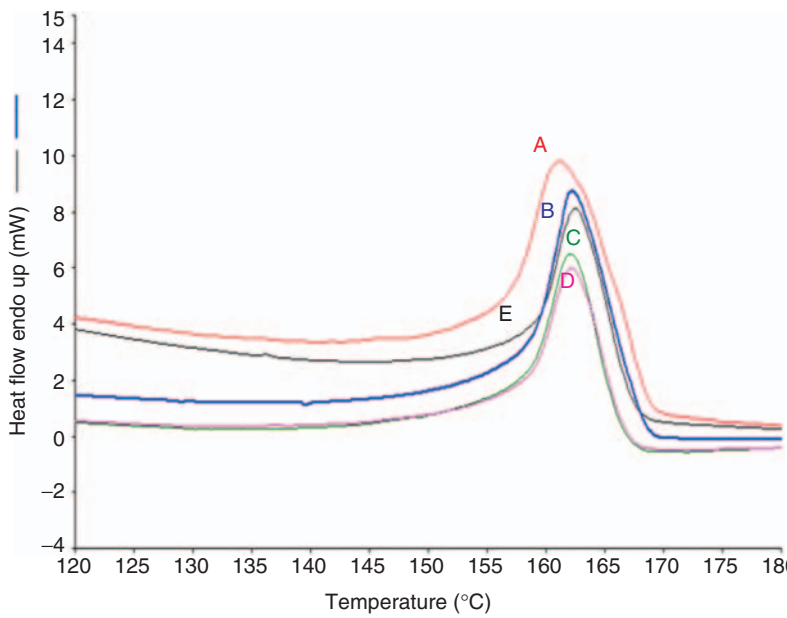

Figure 6. *DSC heating thermograph (a) PP (V), (b) PP + 30%BF, (c) PP + 15%BF + 15%GF, (d) PP + 30%BF + 2%MAPP, (e) PP + 15%BF + 15%GF + 2%MAPP.*

fiber were each investigated using DSC as shown in Figures 6 and 7, respectively. The melting temperature (T_m), crystallization temperature (T_c) and heat of fusion (ΔH_m) for the PP phase in the composites and hybrid composites were determined from the DSC thermograms and are summarized in Table 3. The melting temperature of pure

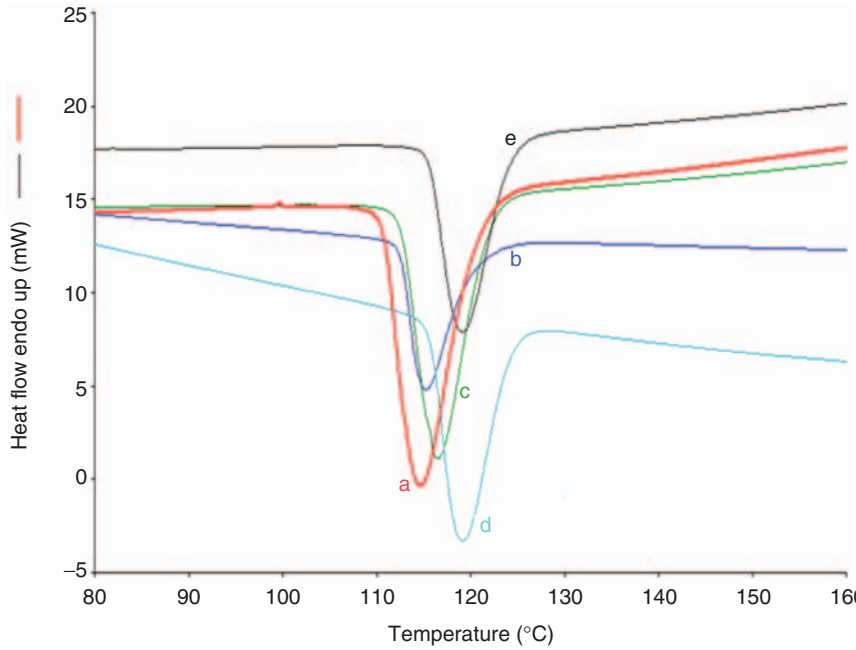

Figure 7. *DSC cooling thermograph of (a) PP (V), (b) PP + 30%BF, (c) PP + 15%BF + 15%GF, (d) PP + 30% BF + 2%MAPP, (e) PP + 15%BF + 15%GF + 2%MAPP.*

Table 3. Melting and crystallization properties.

Sample type	T_m (°C)	T_c (°C)	ΔH_m (J/g)	% X_c
PP	162	116.54	33.82	23.24
BFRP 30%	163.36	118.92	35.52	21.34
BGRP (15:15)	164	117.01	24.75	17.00
BFRP 30% + 2%MAPP	162.54	121.02	23.03	15.84
BGRP (15:15) + 2%MAPP	162.55	120	17.56	12.12

Note: BFRP 30% = 30% BF + PP, BGRP (15:15) = 15% BF + 15%GF, BFRP 30% + 2%MAPP = 30% BF + PP + 2%MAPP, BGRP (15:15) + 2%MAPP = 15% BF + 15%GF + PP + 2%MAPP.

PP is 162°C. The addition of bamboo fiber, glass fiber, and MAPP does not significantly affect the T_m. However, introducing fibers and MAPP interrupts the linear crystallizable sequence of the PP and lowers the degree of crystallization. It can also be seen that the T_c of PP (116.5°C) was shifted to high temperature by adding bamboo and glass fiber due to the nucleation effect of fibers and MAPP. T_c of 2% MAPP treated BFRP and BGRP is found to be more than untreated composition indicating a further enhancement in the nucleation by the coupling agent.

Thermogravimetric Analysis (TGA)

Figure 8 and 9 shows TGA/DTG thermograms of the untreated and treated bamboo fiber and glass fiber, whereas Figure 10 shows the TGA thermograph of virgin PP,

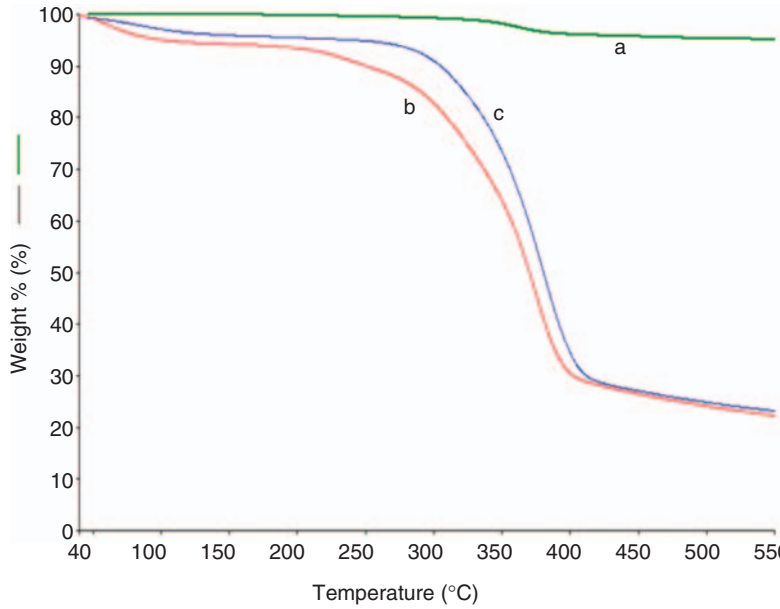

Figure 8. *TGA thermograph fibers (a) glass fiber, (b) untreated bamboo Fiber, (c) untreated bamboo fiber.*

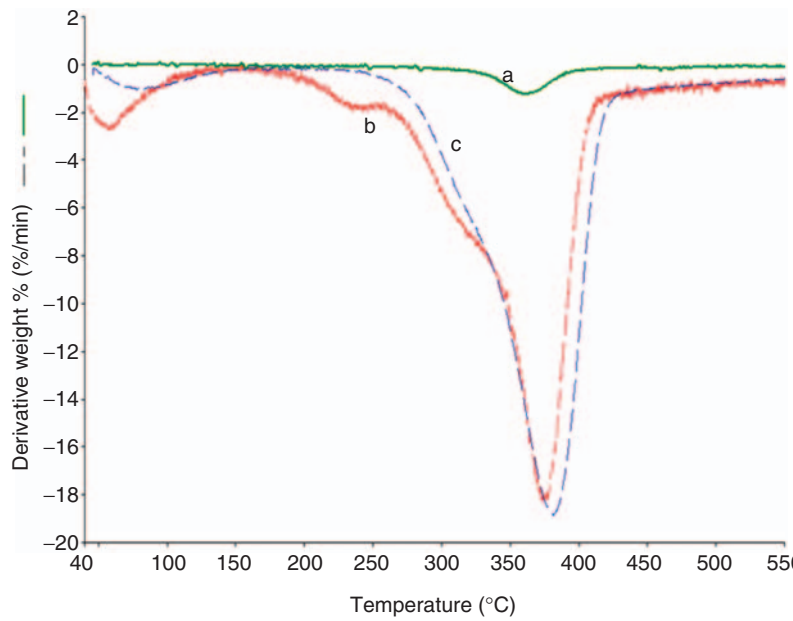

Figure 9. *DTG thermograph Fibers (a) glass fiber, (b) untreated bamboo fiber, (c) untreated bamboo fiber.*

untreated and MAPP treated BFRP and BGRP, respectively, to observe the thermal degradation behavior. A three-stage weight loss of untreated bamboo fiber was observed from the DTG curve (Figure 9), in which the first stage is below 100°C, which is due to the evaporation of the absorbed moisture whereas the second and third stages in the

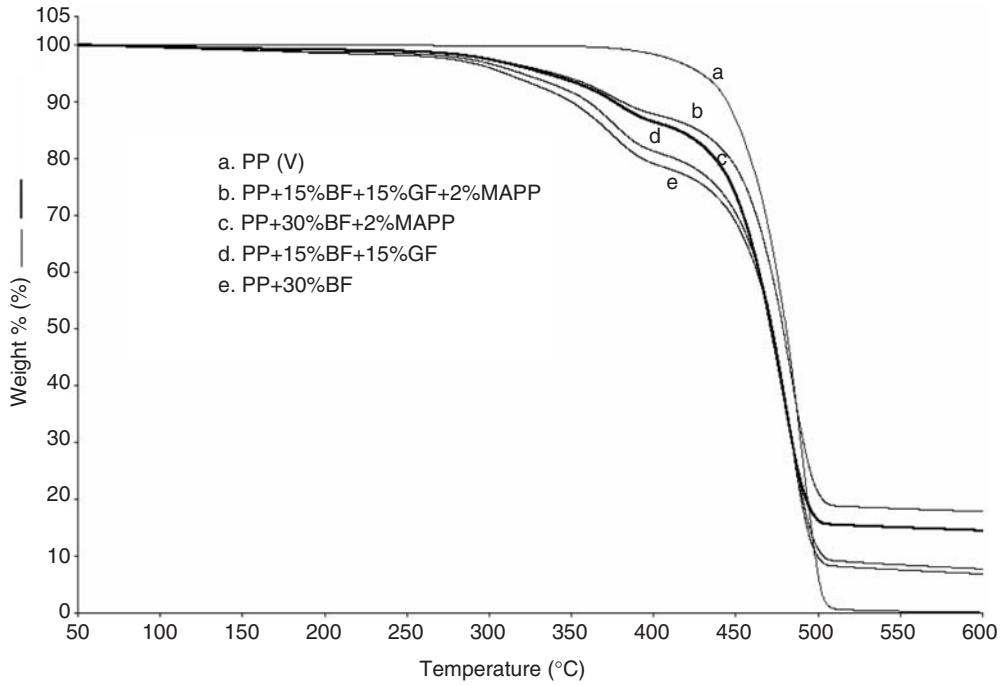

Figure 10. *TGA thermograph of (a) PP (V), (b) PP + 30%BF, (c) PP + 15%BF + 15%GF, (d) PP + 30%BF + 2%MAPP, (e) PP + 15%BF + 15%GF + 2%MAPP.*

temperature range 220–280°C and 350–450°C corresponds to the degradation of low molecular weight hemicelluloses and lignin, respectively. However, only one peak for the decomposition of the cellulose can be detected for MAPP treated bamboo fibers because the MAPP treatment removes the organic gums in the bamboo fibers. These results demonstrate that the presence of MAPP enhances the thermal stability of the bamboo fiber. The higher thermal stability of glass fiber can be identified from a small hump at 400°C on the DTG curve of glass fiber.

The decomposition of virgin PP started at a temperature of 400°C and nearly 100% decomposition occurred at 500°C. In the case of untreated and treated BFRP, a two-stage degradation temperature was observed from which the weight loss at 350°C corresponds to degradation of bamboo fiber, whereas the second stage at 400°C is for the degradation of PP within the untreated BFRP composites. However, the decomposition temperature in both stages for the MAPP treated composites was higher (about 10°C) than that of the composites without coupling agent. This is probably due to the increases in the molecular weight by cross-linking reaction between PP matrix and bamboo fiber. Further, with the incorporation of glass fiber, the thermal stability of both untreated and treated BGRP increases due to the higher thermal stability of glass fiber than bamboo fiber.

Dynamic Mechanical Analysis (DMA)

STORAGE MODULUS (E′)

The comparison of storage modulus as a function of temperature for the untreated and 2 wt% MAPP treated BFRP reinforced with 30 wt% of bamboo fiber, BGRP reinforced

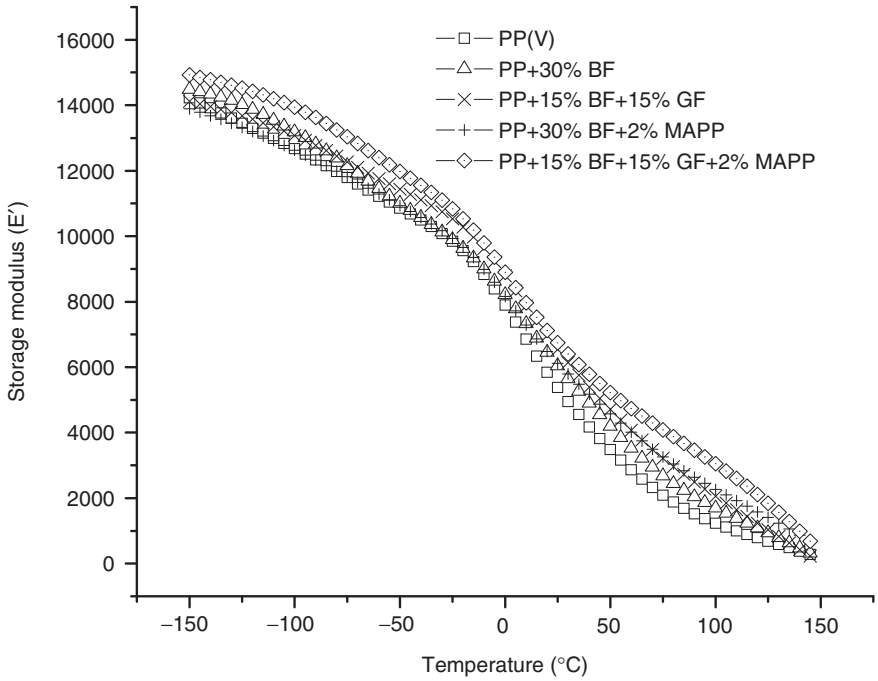

Figure 11. *Storage modulus vs temperature curve.*

with 15:15 wt% of bamboo:glass fiber, and virgin PP, is graphically enumerated in Figure 11. From Figure 11, a decreasing trend in the storage modulus over the whole temperature range is observed and no major transition is detectable. A significant fall of E' was observed in the region between −50 and 100°C. However, with the incorporation of fiber, decrease in E' was compensated by the interaction caused by the reinforcing effect of fibers in the matrix [46]. The storage modulus of virgin PP increased considerably with the incorporation of bamboo fiber. This is mainly attributed to the increase in the stiffness of the matrix due to the reinforcing effect imparted by bamboo fiber that allows greater degree stress transfer from the matrix to the fiber. Addition of glass fiber to the composites further increases E' value due to the hybrid effect caused by the presence of much stiffer glass fibers.

The dynamic mechanical properties are greatly affected by the presence of coupling agents. Better adhesion between the polymer matrix and fiber results in the treated composition, which is evident from improved high temperature modulus and higher softening temperature than the untreated composites. Incorporation of 2% MAPP results in an increase in E' as compared with the uncompatibilized system. This is due to migration of compatibilizer to the fiber surface to form an ester linkage with the fiber with the tail of the compatibilizer showing entanglements with the PP matrix, resulting in a stiffer combination.

LOSS MODULUS (E'')

The variation of loss modulus (E'') of virgin PP, untreated and MAPP treated BFRP and BGRP as a function of temperature is shown in Figure 12. From the graph three transition peaks (α, β, and γ) are observed. The α transition peak corresponds to the

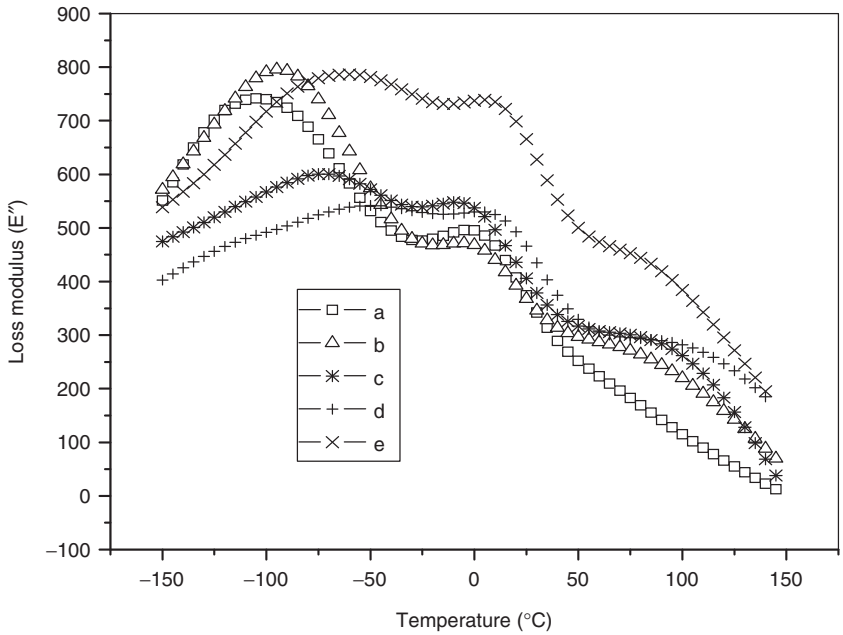

Figure 12. *Loss modulus: (a) PP(V), (b) PP + 30%BF, (c) PP + 15%BF + 15%GF, (d) PP + 30%BF + 2MAPP, and (e) PP + 15%BF + 15%GF + 2%MAPP.*

relaxation of 'rigid amorphous' PP chains in the crystalline phase whereas the β transition is due to the relaxation of unrestricted amorphous PP and corresponds to the glass transition temperature, T_g. The γ transition around –100°C is related to the relaxation of amorphous propylene segments of the PP chain. As seen from Figure 12, the β peak temperature of the MAPP treated BFRP and BGRP is higher than the untreated composition as well as virgin PP, which is probably due to restricted segmental motion of the amorphous polypropylene molecules at the fiber–matrix interface. This suggested that the polymer molecules are more restricted in motion due to the increased fiber–matrix adhesion in the presence of MAPP resulting in less distinct and border transition peaks.

Loss Tangent (tan δ)

In a composite system, tan δ is affected with the incorporation of fibers due to the elastic nature of fiber and shear stress concentrations at the fiber ends, in association with the additional viscoelastic energy dissipation in the matrix material. The fiber–matrix interactions also have a great role in determining the tan δ value. The mobility of the macromolecular chains located in the fiber surface interface reduces with the increase in the fiber–matrix interaction that results in a shift in the glass transition temperature T_g towards higher temperature range and decrease in tan δ [52–56]. Figure 13 delineates the dependence of loss tangent with the temperature for the untreated and treated BFRP and BGRP along with virgin PP. From the plots, the tan δ peak for virgin PP is measured to be -5°C, whereas for all the bamboo fiber reinforced composites, the peaks were located at about 5–10°C. This peak is correlated to the β-relaxation peak of PP and corresponds to the glass transition of the amorphous domains [57]. This maximum peak is assigned as the glass-transition temperature (T_g). The increase in T_g in the PP/bamboo composites is mainly due to the

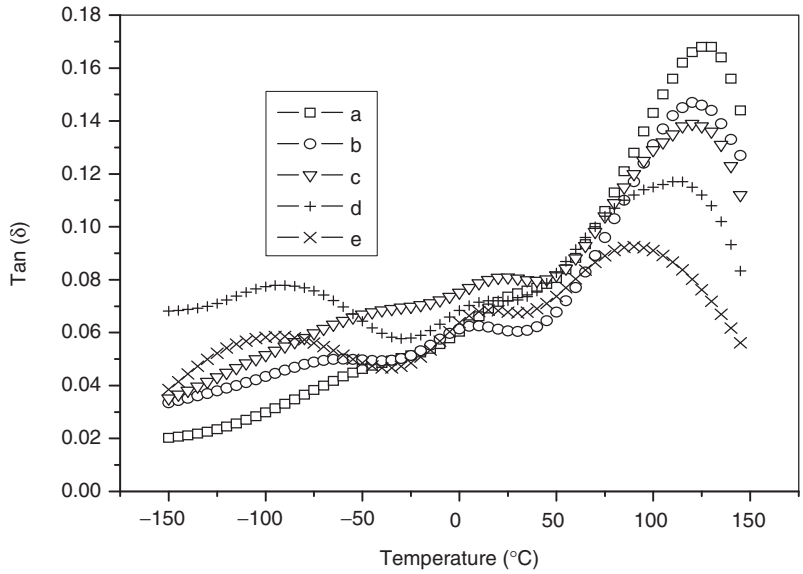

Figure 13. *Tan δ vs temperature: (a) PP (V), (b) PP + 30%BF, (c) PP + 15%BF + 15%GF, (d) PP + 30%BF + 2%MAPP, and (e) PP + 15%BF + 15%GF + 2%MAPP.*

decrease in segmental mobility of the polymer chain. Kuruvilla et al. [58] have also reported that incorporation of short sisal fiber into low-density polyethylene (LDPE), results in an increase in storage and loss modulus, whereas the mechanical loss factor (tan δ) decreases. The tan δ values were lowered in the BFRP and BGRP as compared to the virgin matrix because of the less weight fraction of PP matrix to dissipate the vibrational energy. It can also be seen that there is an additional tan δ peak at about 90°C in the MAPP treated BFRP and BGRP, which corresponds to the T_g of MAPP. A decline in the tan δ values with addition of MAPP indicates an improvement in interfacial bonding in composites because the higher the damping at the interface, the poorer the interface adhesion.

CONCLUSIONS

The mechanical and dynamic mechanical properties of bamboo/PP composites and bamboo-glass/PP hybrid composites have been investigated. It was observed that the composites prepared at 30% fiber loading with 2% MAPP concentration showed optimum mechanical performance. Storage modulus vs. temperature plots showed an increase in the magnitude of the peaks with the addition of fibers and MAPP. The damping properties of the composites, however, decreased with the addition of the fibers and MAPP. Replacement of hydrophilic bamboo fiber by much stronger and stiffer glass fiber not only increases the mechanical properties of the composites but also significantly decreases the water uptake of composites. The improved interaction between bamboo/glass fiber and PP after MAPP treatment also verified from the SEM images of the fractured surface of the composites indicates that MAPP can efficiently improve the fiber–matrix adhesion in the hybrid composites when used at an optimal concentration. Further, DSC and TGA/DTG thermograms also confirmed an increase in thermal stability and crystallization temperature of PP matrix in hybrid composites with the addition of MAPP.

REFERENCES

1. Coutinho, F. M. B., Costa, T. H. S. and Carvalho, D. L. (1997). Polypropylene-wood Fiber Composites: Effect of Treatment and Mixing Conditions on Mechanical Properties, *J. Appl. Polym. Sci.*, **65**: 1227.
2. Schneider, J. P. and Karmaker, A. C. (1995). Composites From Jute- and Kenaf-reinforced Polypropylene, *ANTEC' 95-*, Vol. II – Materials, Boston, Massachusetts, USA, pp. 2086–2090.
3. Mishra, H. K., Dash, B. N., Tripathy, S. S. and Padhi, B. N. (2000). A Study on Mechanical Performance of Jute-Epoxy Composites, *Polym. Plast. Technol. Eng.*, **39**: 187.
4. Mohanty, A. K., Khan, M. A. and Hinrichsen, G. (2000). Influence of Chemical Surface Modification on the Properties of Biodegradable Jute Fabrics–Polyester Amide Composites, *Composites: Part A*, **31**: 143.
5. Tripathy, S. S., Di Landro, L., Fontanelli, D., Marchetti, A. and Levita, G. (2000). Mechanical Properties of Jute Fibers and Interface Strength with an Epoxy Resin, *J. Appl. Polym. Sci.*, **75**: 1585.
6. Rout, J., Mishra, M., Tripathy, S. S., Nayak, S. K. and Mohanty, A. K. (2001). The Influence of Fiber Treatment on the Performance of Coir/Polyester Composites, *Compos. Sci. Technol.*, **61**: 1303.
7. Mishra, S., Mishra, M., Tripathy, S. S., Nayak, S. K. and Mohanty, A. K. (2001). Potentiality of Pineapple Leaf Fibre as Reinforcement in PALF-Polyester Composite: Surface Modification and Mechanical Performance, *J. Reinforced Plastics and Composites*, **20**: 321.
8. Botev, M., Betchev, H., Bikaris, D. and Panayiotou, C. (1999). Mechanical Properties and Viscoelastic Behavior of Basalt Fiber-reinforced Polypropylene, *J. Appl. Polym. Sci.*, **74**: 523.
9. Ray, D., Sarkar, B. K., Das, S. and Rana, A. K. (2002). Dynamic Mechanical and Thermal Analysis of Vinylester-Resin-Matrix Composites Reinforced with Untreated and Alkali-Treated Jute Fibers, *Compos. Sci. Technol.*, **62**: 911–917.
10. Ray, D., Sarkar, B. K., Basak, R. K. and Rana, A. K. (2002). Study of Thermal Behaviour of Alkali-Treated Jute Fibers, *J. Appl. Polym. Sci.*, **85**: 2594–2599.
11. Khan, M. A., Mina, F. and Drzal, L. T. (2000). Influence of Silane Coupling Agents of Different Functionalities on the Performance of Jute-Polycarbonate Composites, *Third International Conference on Wood and natural Fiber Composites Symposium*, pp. 5-1–5-26, Kassel, Germany.
12. Rong, M. Z., Zhang, M. Q., Liu, Y., Zhang, Z. W., Yang, G. C. and Zeng, H. M. (2002). Mechanical Properties of Sisal Reinforced Composite in Response to Water Absorption, *Polym. Polym. Comp.*, **10**(6): 407–426.
13. Pothan, L. A. and Thomas, S. (2003). Polarity Parameters and Dynamic Mechanical Behaviour of Chemically Modified Banana Fiber Reinforced Polyester Composites, *Compos. Sci. Technol.*, **63**: 1231–1240.
14. Herrera-Franco, P. J. and Valadev-Gonzales, A. (2004). Mechanical Properties of Continuous Natural Fiber-Reinforced Polymer Composites, *Composites: Part A*, **35**: 339–345.
15. Khan, M. A., Rahman, M. M. and Akhunzada, K. S. (2002). Grafting of Different Monomers onto Jute Yarn by In Situ UV-Radiation Method: Effect of Additives, *Polym. Plast. Technol. Eng.*, **41**(4): 677–689.
16. Gassan, J. and Gutowski, V. S. (2000). Effects of Corona Discharge and UV Treatment on the Properties of Jute-Fiber Epoxy Composites, *Compos. Sci. Technol.*, **60**(15): 2857–2863.
17. George, J., Bhagawan, S. S. and Thomas, S. (1998). Improved Interactions in Chemically Modified Pineapple Leaf Fiber Reinforced Polyethylene Composites, *Compos. Interf.*, **5**(3): 201–223.
18. Pothan, L. A., George, J. and Thomas, S. (2002). Effect of Fiber Surface Treatment on the Fiber-Matrix Interaction in Banana Fiber Reinforced Polyester Composites, *Compos Interf.*, **9**(4): 335–353.
19. Jones, R. M. (1975). *Mechanics of Composite Materials*, McGraw-Hill, New York.
20. Nielsen, L. E. and Landel, R. F. (1994). *Mechanical Properties of Polymers and Composites*, Marcel Dekker Publishers Ltd, New York.
21. Lai, S. M., Yeh, F. C., Wang, Y., Chan, H. C. and Shen, H. F. (2003). Comparative Study of Maleated Polyolefins as Compatibilizers for Polyethylene/Wood Flour Composites, *J. Appl. Polym. Sci.*, **87**: 487.
22. Keener, T. J., Sturt, R. K. and Brown, T. K. (2004). Maleated Coupling Agents for Natural Fibre Composites, *Composites: Part A*, **35**: 357.
23. George, J., Shreekala, M. S. and Thomas, S. (2001). A Review on Interface Modification and Characterization of Natural Fiber Reinforced Plastic Composites, *Polym. Eng. Sci.*, **41**: 1471.
24. Maiti, S. N., Subbarao, R. and Ibrahim, M. N. (2004). Effect of Wood Fibers on the Rheological Properties of i-PP/wood Fiber Composites, *J. Appl. Polym. Sci.*, **91**: 644.
25. Hou, C., Wang, C. G., Ying, L. and Cai, H.-S. (2004). Affect of Dope Additives on Finishing Behavior Of Carbon Fiber, **90**: 2752.
26. Short, D. and Summerscales, J. (1979). Hybrids - a Review. Part 1: Techniques Design and Construction, *Composites*, **10**: 215–221.

27. Short, D. and Summerscales, J. (1980). Hybrids- A Review. II- Physical Properties (CFRP-GFRP) Composites, *Composites*, **11**: 33–38.
28. Hancox, N. L. (1981). *Fiber Composite Hybrid Materials*, Applied Science Publishers Ltd., London.
29. Kretsis, G. (1987). A Review of the Tensile, Compressive, Flexural and Shear Properties of Hybrid Fiber-Reinforced Plastics, *Composites*, **18**: 13–23.
30. Bunsell, A. R. and Harris, B. (1974). Hybrid Carbon and Glass Fiber Composite, *Composites*, **5**: 157–164.
31. Whan, C. J., Choi, J. S. and Yoon, Y. S. (2002). Electromechanical Behavior of Hybrid Carbon/Glass Fiber Composites with Tension and Bending, *J. Appl. Polym. Sci.*, **83**: 2447.
32. Belingardi, G., Cavatorta, M. P. and Frasca, C. (2006). Bending Fatigue Behavior of Glass–carbon/Epoxy Hybrid Composites, *Compos. Sci. & Tecnol.*, **66**: 222–232.
33. Summerscales, J. and Short, D. (1978). Carbon Fibre and Glass Fibre Hybrid Reinforced Plastics, *Composites*, **9**: 157–166.
34. Shan, Y., Lai, K.-F., Wan K.-T. and Liao, K. (2002). Static and Dynamic Fatigue of Glass-carbon Hybrid Composites in Fluid Environment, *J. Compos. Materials*, **36**: 159–172.
35. Agrawal, D. B. and Broutman, J. L. (1990). *Analysis and Performance of Fiber Composites*, **2nd edn**, Wiley, New York.
36. Stefanidis, S., Mai, Y. W. and Cotterell, B. (1985). The Specific Work of Fracture of Carbon/Kevlar Hybrid Fiber Composites, *J. Materials Sci. Letters*, **4**: 1033–1035.
37. Fisher, S. and Marom, G. (1987). The Flexural Behavior of Aramid Fiber. Hybrid. Composite. Materials, *Compos. Sci. Technol.*, **28**: 291–314.
38. Aronhime, J., Harel, H., Gilbert, A. and Marom, G. (1991). The Rate-dependence of Flexural Shear Fatigue and Uniaxial Compression of Carbon- and Aramid-fiber Composites and Hybrids, *Compos. Sci. Technol.*, **43**: 105–116.
39. Lu, S.-H., Liang, G.-Z., Zhou, Z.-W. and Fang, L. (2006). Structure and Properties of UHMWPE Fiber/Carbon Fiber Hybrid Composites, *J. Appl. Polym. Sci.*, **101**: 1880–1884.
40. Peijs, A. A. J. M. and Venderbosch R. W. (1991). Hybrid Composites Based on Polyethylene and carbon Fibers Part IV Influence of Hybrid Design on Impact Strength, *J. Materials Sci. Letters.*, **10**: 1122–1124.
41. Jang, J. and Moon, S. (1995). Impact Behavior of Carbon Fiber/Ultra-high Modulus Polyethylene Fiber Hybrid Composites, *Polym. Compos.*, **16**: 325–329.
42. Li, Y., Xian, X. J., Choy, C. L., Guo, M. and Zhang, Z. (1999). Compressive and Flexural Behavior of Ultra-high-modulus Polyethylene Fiber and Carbon Fiber Hybrid Composites, *Compos. Sci. Technol.*, **59**: 13–18.
43. Park, R. and Jang, J. (1998). The Effects of Hybridization on the Mechanical Performance of Aramid/Polyethylene Intraply Fabric Composites, *Compos. Sci. Technol.*, **58**: 1621–1628.
44. Park, R. and Jang, J. (1998). Stacking Sequence Effect of Aramid-UHMPE Hybrid Composites by Flexural Test Method, *Polym. Testing*, **16**: 549–562.
45. Ward, I. M. and Ladizesky, N. H. (1985). Ultra High Modulus Polyethylene Composites, *Pure & Appl. Chem.*, **57**: 1641–1649.
46. Joseph, P. V., Mathew, G., Joseph, K., Groeninckx, G. and Thomas, S. (2003). Dynamic Mechanical Properties of Short Sisal Fiber Reinforced Polypropylene Composites, *Composites. Part A, Applied science and Manufacturing*, **34**: 275–290.
47. Jhon, K. and Naidu, S. V. ((2004). Sisal/Glass Fiber Hybrid Composites: The Impact and Compressive Properties, *J. Reinf. Plst. & Composit.*, **23**: 1253.
48. Panthapulakkal, S. and Sain, M. (2007). Studies on the Water Absorption Behavior of short Hemp-Glass Fiber hybrid Polypropylene Composites, *J. Compos. Materials*, **41**: 1871–1883.
49. Kalaprasad, G., Joseph, K. and Thomas, S. (1997). Influence of Short Glass Fiber Addition on the Mechanical Properties of Banana Reinforced Low Density Polyethylene Composites, *J. Comp. Matter*, **31**: 509–526.
50. Kalaprasad, G., Thomas, S., Pavithran, C., Neelakantan, N. R. and Balakrishna, S. (1996). Hybrid Effect in the Mechanical Properties of Short Banana/Glass Hybrid Fiber Reinforced Low Density Polyethylene Composites, *J. Reinf. Plast. Compo.*, **15**: 48–73.
51. Yang, G. C., Zeng, H. M., Jian, N. B. and Li, J. J. (1996). Properties of Banana Fiber/Glass Fiber Reinforced PVC Hybrid Composites, *Plastics Industry*, **1**: 79–81.
52. Ibarra L. and Panos D. (1998). Dynamic Properties of Thermoplastic Butadiene-styrene (SBS) and Oxidized Short Carbon Fiber Composite Materials, *J. Appl. Polym. Sci.*, **67**: 1819.
53. Kodama, M., Karino, I. and Kobayashi, J. (1986). Interaction Between the Reinforcement and Matrix in Carbon-fiber-reinforced Composite: Effect of Forming the Thin Layer of Polyimide Resin on Carbon Fiber by *in situ* Polymerization, *J. Appl. Polym. Sci.*, **32**: 5057.

54. Kubat, J., Rigdahl, M and Welander, M. (1990). Characterization of Interfacial Interactions in High Density Polyethylene Filled with Glass Spheres using Dynamic-mechanical Analysis, *J. Appl. Polym. Sci.*, **39**: 1527.
55. Ko, Y. S., Forsman, W. C. and Dziemianowicz, T. S. (1982). Carbon Fiber-reinforced Composites: Effect of Fiber Surface on Polymer Properties, *Polym. Eng. Sci.*, **22**: 805.
56. Dong, S. and Gauvin, R. (1993). Application of Dynamic Mechanical Analysis for the Study of the Interfacial Region in Carbon Fiber/Epoxy Composite Materials, *Polym. Compos.*, **14**: 414.
57. McCrum, N. G., Read, B. E. and Willians, G. (1967). *Anelastic and Dielectric Effects in Polymeric Solids*, Dover, New York.
58. Kuruvilla, J., Thomas, S. and Pavithran, C. (1993). Dynamic Mechanicanical Properties of Short Sisal Fiber Reinforced Low-density Polyethylene Composites, *J. Reinfor. Plasts. Compos.*, **12**: 139–155.